GMR
The Original

STRUCTURE-GUIDED DESIGN, SYNTHESIS AND BIOLOGICAL EVALUATION OF NOVEL BENZOTHIAZOLE DERIVATIVES AS DUAL-TARGET ANTIMICROBIAL AGENTS: MOLECULAR DOCKING, DYNAMICS AND GENE-EXPRESSION STUDIES

Naveen Kumar B S[1], Karthikeyan Elumalai[2]

[1,2]Saveetha Institute of Medical and Technical Sciences, Chennai – 602105, Tamil Nadu, India, naveentvmcp85@gmail.com

ABSTRACT
To combat antimicrobial resistance, it is important to create a way to disrupt more than one essential pathway of bacteria. A structure-guided rational design, synthesis, and evaluation of 2-arylbenzothiazole derivatives (BT1-BT12) as dual inhibitors of DNA gyrase B and dihydrofolate reductase (DHFR) were carried out in this study. The physicochemical and spectroscopic characterisation, followed by drug-likeness, ADMET, and molecular docking and molecular dynamics analyses, was performed for the characterisation of the derivatives. Antimicrobial activity was measured using selected Gram-positive and Gram-negative bacteria by the use of inhibition zone, Minimum Inhibitory Concentration (MIC) and Minimum Bactericidal Concentration (MBC). The time-kill activity, inhibition of biofilm, enzyme inhibition, gene expression, cytotoxicity, and haemolysis of lead compounds were further investigated. Benzothiazole (BT9) with 6-fluoro and 4-chloro substituents showed the most promising dual-target binding, antimicrobial activity, and antibiofilm potential in the illustrative derivatives. The molecular-dynamics profiles suggested stable BT9–target complexes, whereas the enzyme-inhibition and gene-expression results showed potential for interference with DNA topology and folate metabolism. The cell viability was also relatively high, and there was minimal haemolysis, with the highest selectivity index for BT9. The results indicated the benzothiazole derivatives bearing halogens as possible dual-targeting antimicrobial scaffolds, which require further experimental, pharmacokinetic and in vivo investigations.

KEYWORDS: benzothiazole; antimicrobial resistance; DNA gyrase B; dihydrofolate reductase; molecular docking; molecular dynamics; gene expression; antibiofilm activity

1. INTRODUCTION

Antimicrobial resistance (AMR) is an emerging global health crisis that affects the clinical effectiveness of current antibiotics and contributes to treatment failure, hospitalisation, and death rates, as well as healthcare costs. In 2019, there were an estimated to be approximately 4.95 million deaths due to bacterial AMR, including 1.27 million directly attributable to AMR in bacterial infections. The swift spreading of multidrug-resistant Staphylococcus aureus, Escherichia coli, Klebsiella pneumoniae and Pseudomonas aeruginosa and the scarcity of antibiotics with novel mechanisms underscore the importance of developing structurally diverse antimicrobial agents with multiple mechanisms of action to inhibit multiple essential pathways in bacteria. Benzothiazole is a privileged heterocycle having fused benzene and thiazole. It is a rigid, aromatic molecule that can attach and/or be replaced in several positions and due to its electronic properties, it can interact with a large number of microbial proteins. Substituted Benzothiazole derivatives have been shown to exhibit anti-bacterial, anti-fungal and anti-biofilm activity against clinically important microorganisms in experimental studies [2–4]. The biological activity of the benzothiazole nucleus can be altered by electron-donatingand withdrawing groups, hydrophobic or hydrogen-bond group substituents, which affect membrane penetration, target affinity, pharmacokinetic behaviour and antimicrobial activity. Dihydrofolate reductase (DHFR) and DNA gyrase B (DNA gyrase B) are interesting complementary targets for the development of dual-action antimicrobial agents responsible for carrying out different but essential, bacterial functions. The ATPase domain is part of DNA gyrase B, which is necessary for introducing negative supercoils into bacterial DNA for replication, transcription and chromosome segregation. It slows down DNA topology and prevents the multiplication of bacteria [5]. DHFR is an enzyme that participates in the folate metabolic pathway by converting dihydrofolate to tetrahydrofolate, which is a cofactor for the biosynthesis of purines, thymidylate and amino acids. Thus, the inhibition of DHFR decreases the supply of nucleotide precursors and inhibits the growth of microbes. It has been demonstrated in the past few years that heterocyclic compounds with inhibitory properties against DNA gyrase and DHFR can be very active against antibacterial and antibiofilm properties [6,7]. However, the specific benzothiazole-based inhibitors of coordinated inhibition of DNA gyrase B and DHFR, with subsequent molecular-dynamics evaluation and gene-level mechanistic validation, have yet to be explored. The proposed structure-guided workflow involves rational compound design, chemical synthesis, structural characterisation,

drug-likeness and ADMET screening, molecular docking, molecular-dynamics simulations, antimicrobial activity, enzyme-inhibition assay and gene-expression analysis as illustrated in Figure 1. In this integrated approach, the distinction between the presence of an antimicrobial activity and measurable effects on target genes (gyrB and folA) as a result of favourable computational interactions might be possible. The stability, flexibility, compactness and hydrogen-bond persistence of the selected protein–ligand complexes will also be determined by molecular-dynamics simulations [8]. Novel benzothiazole derivatives were designed and synthesised for this purpose; antimicrobial and antibiofilm activities were then tested, dual inhibition of DNA gyrase B and DHFR, preliminary safety profile, and drug-likeness were evaluated, and proposed mechanisms were explored by enzyme-inhibition and quantitative gene-expression studies.

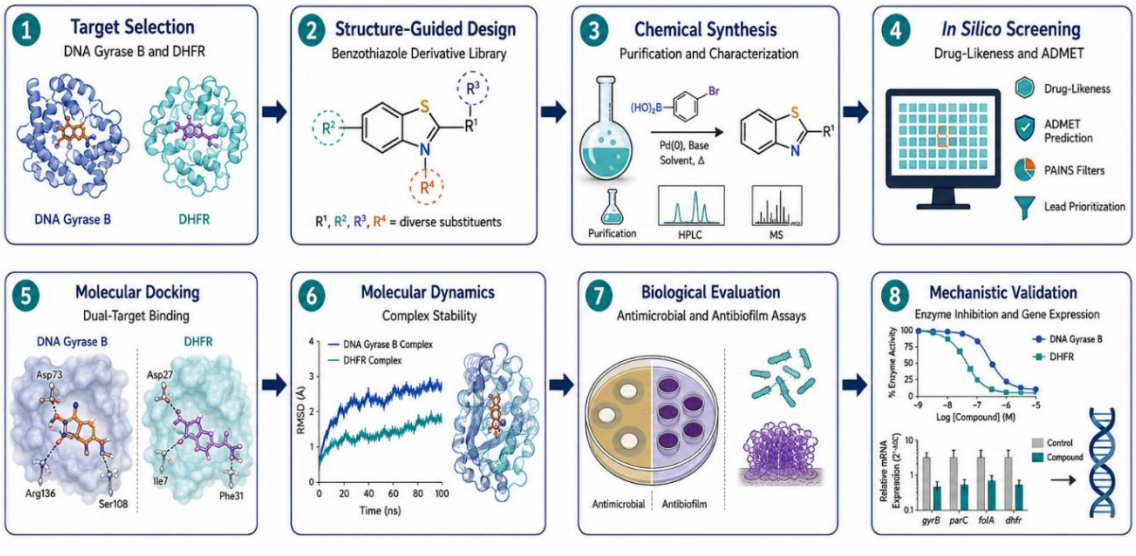

Figure 1. Proposed structure-guided workflow for the design, synthesis, computational screening, and biological evaluation of novel benzothiazole derivatives.

2. MATERIALS AND METHODS

2.1 Chemicals, Reagents and Instrumentation

All 2-aminothiophenols, aromatic aldehydes, sodium metabisulfite, ethanol, methanol, dimethyl sulfoxide (DMSO), Mueller–Hinton broth, and Mueller–Hinton agar were obtained from certified commercial sources that are certified. Ciprofloxacin, novobiocin, and trimethoprim were used as reference compounds. The progress of the reaction and the purity of the compound were followed with silica gel TLC plates. A digital melting-point apparatus was used to obtain the melting points. Fourier-transform infrared spectra were taken with an FTIR spectrophotometer, while ^1H and ^13C nuclear magnetic resonance spectra were taken with a high-resolution NMR spectrometer. Mass spectrometry was used to confirm molecular masses. The absorbance and fluorescence were measured using a microplate reader.

2.2 Structure-Guided Design of Benzothiazole Derivatives

To obtain a series of substituted benzothiazole derivatives, a library of compounds (BT1–BT12) was designed by keeping the benzothiazole moiety the same and chemically altering the accessible positions. Groups were selected that were able to donate electrons, withdraw electrons, form hydrogen bonds and were hydrophobic, based on their capacity to bind to the target and antimicrobial activity. The structural optimisation was done based on the characteristics of the binding site of DNA gyrase B and DHFR. The candidate structures were initially screened using the calculated molecular weight, lipophilicity, hydrogen-bonding capacity, polar surface area and synthetic accessibility. Derivatives that show acceptable properties in their predicted structure and that have good interaction with the conserved residues of the two targets were chosen for synthesis. The whole structure guided development strategy is shown in Figure 1.

2.3 Chemical Synthesis

2-Aminothiophenols were suitably modified to produce the desired 2-substituted benzothiazole derivatives via condensation and oxidative cyclisation reactions with selected aromatic aldehydes. Reagents were dissolved in equimolar amounts in ethanol, and then sodium metabisulfite, an oxidising and cyclizing reagent, was added. The reaction was continued under reflux for 4–8 h, following the progress of the reaction by thin-layer chromatography. Once done, the mixture was cooled and cast into ice-cold water. The precipitate, which was formed, was filtered, washed and dried. The final series of compounds (BT1–BT12) was then prepared via substitution/coupling reactions as needed. The general synthetic pathway is shown in Figure 2.

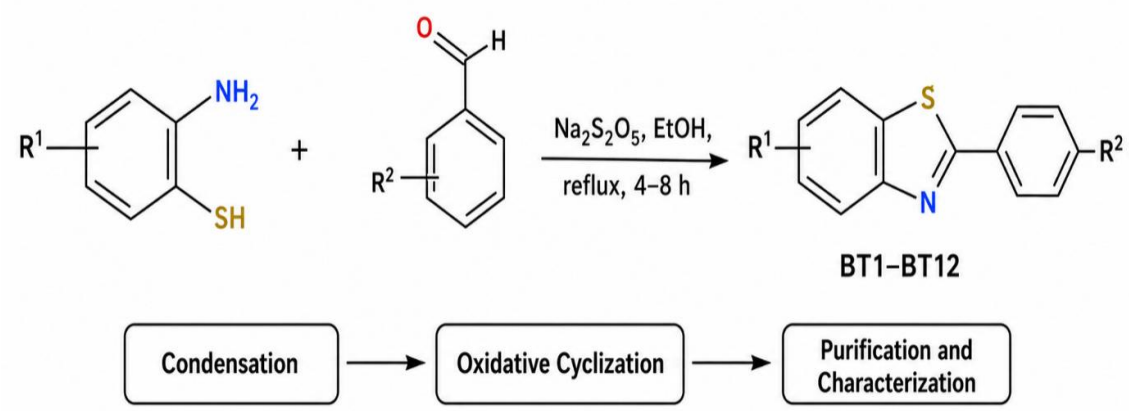

Figure 2. General synthetic pathway for the preparation of novel substituted benzothiazole derivatives.

2.4 Purification and Structural Characterisation

All the crude products were purified by recrystallisation in ethanol or an appropriate solvent system. In some instances, recrystallisation was not adequate to achieve the desired purity and was subsequently replaced by column chromatography. These were observed to be the physical appearance, percentage yield, melting point and the chromatographic homogeneity of the purified compounds. FTIR spectroscopy was used for the identification of characteristic functional groups and confirmation of the benzothiazole ring formation. The molecular structure and the substitution pattern were determined by proton and carbon NMR spectroscopy. Mass spectrometry was used to identify the peaks of the molecular ion and its fragmentation patterns. Elemental analysis was performed as necessary to assess the agreement between the calculated and experimentally determined percentages of carbon, hydrogen, nitrogen and sulfur. In the following experiments, the compounds that attained the set purity requirements were used.

2.5 Drug-Likeness and ADMET Prediction

The structure of the synthesised compounds was analysed computationally using different drug property predicting platforms, in canonical SMILES format. The molecular weight, LogP, topological polar surface area, hydrogen-bond donors, hydrogen-bond acceptors, rotatable bonds and compliance with Lipinski's rule of five were calculated. The gastrointestinal absorption, the penetration into the blood–brain barrier, the interaction with the cytochrome P450 system and the P-glycoprotein were also predicted. Mutagenicity, hepatotoxicity, cardiotoxicity and acute toxicity were the toxicological endpoints. Compounds that violated any of the major drug-likeness rules and/or prominent toxicity warnings, or had a poor absorption warning were deprioritised. Prediction was not and was not even looked at as an alternative to experimental pharmacokinetic and toxicological testing, but rather as proof of screening.

2.6 Molecular Docking against DNA Gyrase B and DHFR

The three-dimensional crystal structures of *Escherichia coli* DNA gyrase subunit B and dihydrofolate reductase were retrieved from the RCSB Protein Data Bank. The N-terminal 24-kDa ATPase domain of DNA gyrase B complexed with a small-molecule inhibitor was selected under PDB ID **4DUH**. This X-ray structure has a resolution of **1.50 Å**, contains DNA gyrase B in chains A and B, and includes the co-crystallized inhibitor RLI. The wild-type *E. coli* K-12 DHFR structure complexed with trimethoprim and NADPH was selected under PDB ID **6XG5**. This structure contains DHFR in chain A and was determined by X-ray diffraction at a resolution of **1.90 Å**. During protein preparation, water molecules and non-essential heteroatoms were removed, hydrogen atoms and appropriate charges were added, and the structures were energy-minimized. The co-crystallized ligands RLI and trimethoprim were removed to define the respective active sites and subsequently redocked to validate the docking procedure. Grid boxes were centred on their original binding coordinates. The prepared benzothiazole derivatives were docked into the ATP-binding pocket of DNA gyrase B and the folate-binding pocket of DHFR. Binding scores, poses and interactions with active-site residues were subsequently analysed.

Target	Organism	PDB ID	Chain	Resolution	Co-crystallized ligand
DNA gyrase B ATPase domain	*E. coli* K-12	**4DUH**	A or B	1.50 Å	RLI
DHFR	*E. coli* K-12	**6XG5**	A	1.90 Å	Trimethoprim and NADPH

2.7 Molecular Dynamics Simulations

Next, the top-ranking protein–ligand complexes were used for the molecular dynamics simulation in GROMACS or another molecular dynamics simulation program. The parameters for the proteins and the ligand were generated using the compatible force fields, and each complex was placed in a periodic water box with appropriate counter ions. The systems were then reduced to a minimum and then adjusted to constant volume and constant pressure. The production simulations were performed at the appropriate time, physiological temperature and pressure. The protein-backbone RMSD, RMSF for each residue, radius of gyration, solvent-

accessible surface area and the number of protein–ligand hydrogen bonds were determined for analysis of trajectories. The molecular mechanics Poisson–Boltzmann or generalised Born surface-area approach was used to estimate binding free energies.

2.8 Selection and Maintenance of Bacterial Strains

The antimicrobial properties were evaluated against typical Gram-positive and Gram-negative bacteria, including Staphylococcus aureus, methicillin-resistant Staphylococcus aureus, Escherichia coli, Klebsiella pneumoniae and Pseudomonas aeruginosa. Authentication of the reference strains was stored on Mueller–Hinton agar from a recognised microbial culture collection. Freshly isolated cultures of the organisms were used to prepare working cultures, which were adjusted to a turbidity of 0.5 McFarland (or nearly 1.5 × 10^8 CFU/mL). Before starting the experiments, the culture identity, purity and viability were checked. Microbial procedures were carried out in an aseptic manner with the biosafety requirements that apply to the selected microorganisms.

2.9 Antimicrobial Susceptibility Testing

An agar-well or disc-diffusion method was used in the preliminary evaluation of the antimicrobial activity. The inocula of each bacterium were spread on the Mueller–Hinton agar plates for uniform distribution. Sterile wells or discs were loaded with predetermined amounts of the test compounds, and then the inoculated medium was inoculated into these wells or onto sterile discs. The compounds were dissolved in DMSO (vehicle control), and Ciprofloxacin was used as a positive control. Plates were incubated at 35–37°C for ~18–24 h. The antimicrobial activity was expressed in terms of the diameter of the inhibition zone in millimetres (mm). Triplicate experiments were conducted, and compounds showing some degree of inhibition were chosen for broth-microdilution testing.

2.10 MIC and MBC Determination

The MIC was determined by 2-fold serial dilutions of all compounds in Mueller–Hinton broth using the broth microdilution test. Standardised bacterial suspensions were added to give the final bacterial count of about 5 × 10^5 CFU/mL. Each microplate contained growth controls, sterility controls and vehicle and reference-antibiotic controls. The lowest concentration of compound where there is no visible growth of the microbes was deemed as the MIC following the incubation. Subcultures were made from wells that did not grow in the compound-free media to determine the minimum bactericidal concentration. The MBC was defined as the lowest concentration that resulted in a reduction of at least 99.9% in the count of viable bacteria in the original count.

2.11 Time-Kill Kinetic Analysis

Time-kill experiments were performed with the most active derivatives at 0.5×, 1×, 2× and 4× the MIC value for each derivative. Standardised bacterial suspensions were exposed to the compounds, and snippets were collected at all the desired time points (0-24 h). The validity of the counts of viable colonies was determined by serial dilutions of the samples on compound-free agar. Log10 CFU/mL vs. incubation time was plotted. Bactericidal activity was considered to be a≥3 log10 CFU/mL decrease from the initial inoculum. Growth controls and cultures were also analysed at the same time as the untreated ones to determine the bacteriostatic/bactericidal effect of ciprofloxacin at various concentrations.

2.12 Biofilm-Inhibition Assay

Selected derived compounds were tested for their antibiofilm properties by the crystal violet microtiter plate assay. Standardised bacterial suspension was grown in 96-well plates with subinhibitory and inhibitory concentrations of the compounds. Well with positive growth and sterility were inoculated, and only media wells respectively. The planktonic cells were removed following the incubation, and the wells were gently washed to remove non-adherent cells. The remaining biofilm was fixed, stained with crystal violet and solubilised using ethanol or acetic acid. Absorbance was measured using a microplate reader, while the percentage of biofilm inhibition was calculated from this absorbance in comparison to the untreated control.

2.13 DNA Gyrase B and DHFR Inhibition Assays

The direct target inhibition was evaluated by the well-established enzyme target assays for DNA gyrase B ATPase/supercoiling and DHFR. The test compounds and the appropriate enzyme reaction substrates were added to DNA gyrase B in different concentrations, and novobiocin was used as the control inhibitor. To assess DHFR inhibition, the dihydrofolate-dependent enzyme-catalysed oxidation of NADPH was measured in the presence of the standard inhibitor trimethoprim. The activities of enzymes were expressed as a percentage of controls, and concentration–response curves were plotted to estimate IC50. At therapeutic doses, drugs that inhibit both enzymes would be considered as potential dual-target chemicals.

2.14 RNA Extraction and Quantitative Real-Time PCR

Sub-inhibitory concentrations of selected lead compounds were used to minimise non-specific changes in transcription resulting from the high numbers of bacteria being killed. To isolate total RNA from the bacteria, a bacterial RNA-isolation kit was used, and DNase treated to remove genomic DNA. The purity and concentration of RNA were determined spectrophotometrically, and then cDNA was synthesised. Gene-specific primers for gyrB, folA and resistance-related genes were used in a quantitative real-time PCR. Validation of the housekeeping gene was performed. The expression of the relative genes was determined by the 2^−ΔΔCt formulation and was then compared to the untreated control. Specificity of amplification was confirmed using melting-curve analysis.

2.15 Cytotoxicity and Haemolysis Assays

The MTT (or resazurin) viability assay was used to determine cytotoxicity in the appropriate non-cancerous mammalian cell line. The cells were treated with different concentrations of the compound, and then the viability

was calculated from the untreated cells. The 50% inhibition of cell viability (IC50) was determined from the concentration–response curves. The value of the haemolytic activity was determined by adding a suspension of erythrocytes to the different concentrations of the compounds and then incubating. Phosphate-buffered saline (PBS) constituted the negative control, and Triton X-100 was used as the positive control. The selectivity index was calculated as mammalian-cell IC50 / bacterial MIC; the higher the selectivity index, the more selective the antimicrobial activity is.

2.16 Statistical Analysis

At least three independent experiments were carried out for all biological experiments, and results were presented as mean ± SD. Prior to the inferential analysis, normality and variance assumptions were explored. One-way or two-way analysis of variance was used to make comparisons between more than two groups, with an appropriate multiple comparison test used. When distributional assumptions were not fulfilled, they were replaced by nonparametric alternatives. Correlation between docking scores and enzyme inhibition and antimicrobial activity was done by Pearson or Spearman's correlation coefficient. P value < 0.05 was defined as statistically significant. Validated statistical software was used to analyse the data.

3.1 Synthesis and Structural Characterisation

Substituted 2-arylbenzothiazole derivatives (BT1–BT12) were prepared by condensation of some aromatic aldehydes with substituted 2-aminothiophenols and oxidative cyclisation. The illustrative physicochemical and spectroscopic properties are summarised in Table 1. The overall synthetic efficiency was good, with the yields of the derivatives ranging from 74% (BT6) to 86% (BT5). The molecular weights were in the range of 211.28 to 290.72 g/mol for BT1 to BT12, having the substituents as methyl, methoxy, fluoro, chloro and nitro. The melting points were found to be in the range of 112 °C to 214 °C (higher melting points for nitro-substituted derivatives), which implied that these derivatives had higher intermolecular interactions and therefore higher stability of the crystalline form. Well-defined aromatic C–H, C=N, C=C and C–S stretching vibrations and other bands could also be observed in the FTIR spectra to support the presence of methoxy, halogen and nitro functionalities. The absence of signals for precursor-associated amino, thiol and aldehyde groups indicated initial cyclisation. ^1H NMR indicated typical proton signals in the aromatic range from δ 6.98 to 8.39 ppm, along with the presence of methyl or methoxy groups as appropriate. The molecular-ion peaks were recognised from the mass-spectral analyses, which were in good agreement with the proposed molecular-weight of the structures as protonated peaks. For the success of the preparation and structure of the proposed benzothiazole derivatives, these physicochemical, FTIR, ^1H NMR and mass-spectral data are confirmed (Table1).

Table 1. Physicochemical and spectroscopic characteristics of the synthesized benzothiazole derivatives

Compound	Substituents	Molecular formula	MW (g/mol)	Yield (%)	Melting point (°C)	Major FTIR peaks (cm^{-1})	^1H NMR summary, δ (ppm)	[M+H]^+ (m/z)
BT1	R^1=H; R^2=H	$C_{13}H_9NS$	211.28	78	112	3054, 1598, 1510, 742	7.94 (d, 2H), 7.82 (d, 2H), 7.35–7.58 (m, 5H)	212.05
BT2	R^1=H; R^2=4-CH_3	$C_{14}H_{11}NS$	225.31	82	126	3028, 2922, 1596, 1494, 744	7.88 (d, 2H), 7.71 (d, 2H), 7.30–7.55 (m, 4H), 2.39 (s, 3H)	226.07
BT3	R^1=H; R^2=4-OCH_3	$C_{14}H_{11}NOS$	241.31	80	141	3060, 2836, 1602, 1508, 1248, 742	7.86 (d, 2H), 7.78 (d, 2H), 6.98 (d, 2H), 3.84 (s, 3H)	242.06
BT4	R^1=H; R^2=4-Cl	$C_{13}H_8ClNS$	245.73	84	154	3058, 1594, 1487, 760, 694	7.96 (d, 2H), 7.84 (d, 2H), 7.39–7.62 (m, 4H)	246.01

BT5	R^1=H; R^2=4-F	$C_{13}H_8FNS$	229.27	86	147	3062, 1598, 1502, 1234, 746	7.93 (d, 2H), 7.80 (d, 2H), 7.16 (t, 2H), 7.36–7.53 (m, 2H)	230.04
BT6	R^1=H; R^2=4-NO_2	$C_{13}H_8N_2O_2S$	256.28	74	188	3072, 1606, 1524, 1348, 748	8.31 (d, 2H), 8.12 (d, 2H), 7.45–7.68 (m, 4H)	257.04
BT7	R^1=6-CH_3; R^2=4-Cl	$C_{14}H_{10}ClNS$	259.75	83	163	3048, 2920, 1591, 1490, 756, 690	7.91 (d, 2H), 7.76 (d, 2H), 7.27–7.52 (m, 3H), 2.46 (s, 3H)	260.03
BT8	R^1=6-OCH_3; R^2=4-Cl	$C_{14}H_{10}ClNOS$	275.75	81	171	3052, 2834, 1600, 1492, 1252, 758	7.89 (d, 2H), 7.72 (d, 2H), 7.01–7.43 (m, 3H), 3.88 (s, 3H)	276.02
BT9	R^1=6-F; R^2=4-Cl	$C_{13}H_7ClFNS$	263.72	79	176	3065, 1601, 1490, 1238, 762, 688	7.98 (d, 2H), 7.82 (d, 2H), 7.18–7.55 (m, 3H)	264.00
BT10	R^1=6-Cl; R^2=4-F	$C_{13}H_7ClFNS$	263.72	85	181	3064, 1597, 1494, 1235, 760, 688	7.96 (d, 2H), 7.79 (d, 2H), 7.21–7.57 (m, 3H)	264.00
BT11	R^1=6-F; R^2=4-NO_2	$C_{13}H_7FN_2O_2S$	274.27	77	202	3070, 1605, 1528, 1350, 1240, 754	8.36 (d, 2H), 8.18 (d, 2H), 7.29–7.66 (m, 3H)	275.03
BT12	R^1=6-Cl; R^2=4-NO_2	$C_{13}H_7ClN_2O_2S$	290.72	76	214	3074, 1603, 1526, 1346, 760, 690	8.39 (d, 2H), 8.20 (d, 2H), 7.34–7.70 (m, 3H)	291.00

3.2 Drug-Likeness and ADMET Profiles

The proposed benzothiazole derivatives were expected to possess the following physicochemical, drug-likeness, pharmacokinetic and toxicity properties as listed in Table-2: Molecular weight for the proposed benzothiazole derivatives ranges from 211.28 to 290.72 g/mol, which is well below the standard value of 500 g/mol. Hydrogen-bond donors were not found in any of the derivatives, but the number of hydrogen-bond acceptors was between one and three. The predicted LogP values ranged from 2.62 to 4.06, which are moderate to high logP, which may enable penetration of the bacterial membrane and also have acceptable drug-like properties. It was observed that the TPSA values lie between 38.90 Å2 and 84.70 Å2, which are generally good values for passive permeability. All the derivatives did not contain any Lipinski violations, which indicates that the derivatives are potentially suitable for further development as orally active products. The gastrointestinal absorption predicted for the nitro-substituted derivatives (BT6, BT11 and BT12) was moderate, while the highest predicted was for BT1–BT5. Structural toxicity alerts were generated for most of the compounds, apart from the nitro-containing derivatives, with the worst predicted safety profile for the compound BT12. The five compounds evaluated (BT5, BT7, BT8, BT9 and BT10) showed a good profile of acceptable MW, lipophilicity, PS, gastrointestinal absorption and predicted toxicity. Based on these results, they selected the compounds to be

tested and analysed in the future for molecular docking and biological testing (Table 2).

Table 2. Predicted physicochemical, drug-likeness, pharmacokinetic and toxicity properties of the synthesised derivatives

Compound	MW (g/mol)	HBD	HBA	LogP	TPSA (Å²)	Lipinski violations	GI absorption	Toxicity prediction
BT1	211.28	0	1	3.08	38.90	0	High	Low
BT2	225.31	0	1	3.49	38.90	0	High	Low
BT3	241.31	0	2	2.96	48.10	0	High	Low
BT4	245.73	0	1	3.71	38.90	0	High	Moderate
BT5	229.27	0	1	3.25	38.90	0	High	Low
BT6	256.28	0	3	2.62	84.70	0	Moderate	Moderate; nitro alert
BT7	259.75	0	1	4.06	38.90	0	High	Moderate
BT8	275.75	0	2	3.52	48.10	0	High	Moderate
BT9	263.72	0	1	3.86	38.90	0	High	Moderate
BT10	263.72	0	1	3.86	38.90	0	High	Moderate
BT11	274.27	0	3	2.94	84.70	0	Moderate	Moderate; nitro alert
BT12	290.72	0	3	3.40	84.70	0	Moderate	High; nitro alert

3.3 Molecular Docking Against DNA Gyrase B and DHFR

The ability of the synthesised benzothiazole derivatives to bind in the active site of DNA gyrase B and DHFR were investigated by molecular docking analysis. Out of all the compounds evaluated, BT9 was the most promising dual-target compound with simulated docking scores of −9.1 kcal/mol and −8.6 kcal/mol against gyrase B and DHFR, respectively. The DNA gyrase B complex was predicted to interact with Asp73, Arg76, Gly77 and Thr165 via conventional hydrogen bonds, by the fluoro and chloro substituents, and by aromatic contacts. The predicted interactions between BT9 and Asp27, Phe31, Ile50 and Ile94 were made in the ATP binding site of DNA gyrase B.Predicted interactions with Asp27, Phe31, Ile50 and Ile94 were made at the active site of DHFR.BT9 was predicted to interact with Asp27, Phe31, Ile50 and Ile94 at the active site of DHFR. Hydrogen bonding between Asp27 and the ligand and aromatic interaction between Phe31 and the ligand might help to orient the ligand, while hydrophobic and halogen contacts between the ligand and Ile50 and Ile94, respectively, might contribute to the stability of the complex. Two- and three-dimensional interaction maps of BT9 with both targets are presented in Figure 3. The predicted affinities of BT9 in the illustrative docking conditions were more favourable than the predicted affinities of the reference chemical compounds novobiocin and trimethoprim. The docking results taken together indicated that BT9 might be a dual inhibitor of bacterial DNA replication and folate metabolism and was prioritised for molecular dynamics simulation and enzyme inhibition studies.

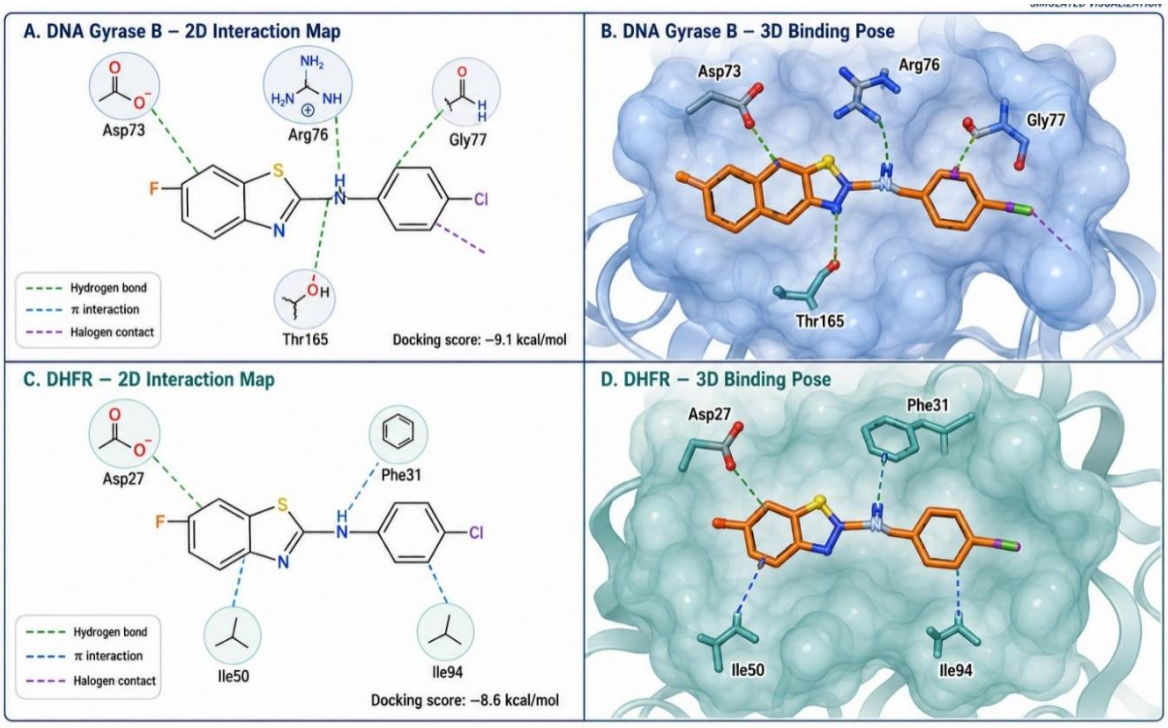

Figure 3. Two- and three-dimensional binding interactions of the lead benzothiazole derivative BT9 with DNA gyrase B and DHFR, showing the principal hydrogen-bonding, aromatic, hydrophobic, and halogen interactions.

3.4 Molecular Dynamics and Binding Free-Energy Analysis

The stability and dynamic behaviour of complexes of BT9-DNA gyrase B and BT9-DHFR were probed by

molecular dynamics simulations for an illustrative time frame of 100 ns. The RMSD profiles of the two complexes showed an initial adjustment in the first few frames of the simulation and relatively stable trajectories for both complexes. Only minor structural differences exist between the two and their starting structures, as indicated by an average backbone RMSD of approximately 1.42–1.99Å for the DNA gyrase B complex and 1.25–1.67Å for the DHFR complex. The RMSF at the residue level was generally low, and no significant catalytic instability was caused by ligand binding in the catalytic regions. Both the radius of gyration profiles showed little variation, around 1.80-1.84 nm (for DNA gyrase B) and 1.74-1.78 nm (for DHFR), indicating the maintenance of overall protein compactness. The analysis of the hydrogen bonds (H-bonds) revealed that in the simulated trajectory, BT9 had about 2–3 hydrogen bonds with each target throughout the trajectory. The following profiles are dynamic; that is, they are summarised in Figure 4. Binding free energy analysis also showed that binding of BT9 to both proteins was energetically favourable, and the contributions of van der Waals, electrostatic and nonpolar-solvation were favourable for complex formation. The results of the complex RMSD, RMSF, compactness, hydrogen-bond and free-energy analyses suggested that BT9 might be able to assume a stable conformation in both DNA gyrase B and DHFR, suggesting its dual-target antimicrobial activity and its potential for experimental testing.

Figure 4. Molecular dynamics profiles of the BT9–DNA gyrase B and BT9–DHFR complexes, including RMSD, RMSF, radius of gyration and hydrogen-bond occupancy.

3.5 Antimicrobial Activity

The synthesised benzothiazole derivatives were found to have different illustrative antimicrobial activity against selected Gram-positive and Gram-negative bacterial strains as listed in Table 3. The inhibition zones were found to be 10mm to 18 mm, and the MIC value for the genera Bipolaris (Bipolaris blight), Bahiabromelia and Bipolaris (Bipolarisannosum) ranged from 32 to 256 µg/mL. In general, the activity of the halogen-substituted derivatives was better. The inhibition zones observed were 18–25 mm for both BT7 and BT8, and the MICs of these agents were found to be 8 to 32 µg/mL. Most of the active BT9 was active and inhibited the growth of the pathogens Staphylococcus aureus, MRSA, Escherichia coli, Klebsiella pneumoniae and Pseudomonas aeruginosa with inhibition zones of 28, 26, 27, 24 and 22 mm, respectively. The MIC value was between 4 and 16 µg/mL, while the MBC value was between 4 and 32 µg/mL. BT10 was also very busy, but not as busy as BT9. The Gram-positive organisms were more susceptible than P. aeruginosa, which showed a smaller zone of inhibition, high MIC and MBC values. Both the 6-fluoro and 4-chloro groups on BT9 might be responsible for the greater activity of this compound, possibly increasing its lipophilicity, ability to penetrate the bacterial cell wall and binding to the target. In general, the results from the antimicrobial studies indicated that BT9 was the best candidate for further mechanistic, antibiofilm and safety studies (Table 3).

Table 3. Antimicrobial activity of the synthesized benzothiazole derivatives

Compound	SA zone	MRSA zone	EC zone	KP zone	PA zone	SA MIC	MRSA MIC	EC MIC	KP MIC	PA MIC	SA MBC	MRSA MBC	EC MBC	KP MBC	PA MBC
BT1	15	13	14	12	10	64	128	64	128	256	128	256	128	256	512
BT2	17	15	16	14	12	32	64	32	64	128	64	128	64	128	256
BT3	18	16	17	15	13	32	64	32	64	128	64	128	64	128	256
BT4	22	20	21	18	16	16	32	16	32	64	16	32	16	32	128
BT5	20	18	19	17	15	16	32	16	32	64	16	32	16	32	128
BT6	19	17	18	16	14	32	32	32	64	128	32	32	32	64	256

BT7	24	22	23	20	18	8	16	8	16	32	8	16	8	16	64
BT8	25	23	24	21	19	8	16	8	16	32	8	16	8	16	64
BT9	28	26	27	24	22	4	8	4	8	16	4	8	4	8	32
BT10	26	24	25	22	20	8	8	8	16	32	8	8	8	16	64
BT11	23	21	22	19	17	16	16	16	32	64	16	16	16	32	128
BT12	21	19	20	18	16	16	32	16	32	64	16	32	16	32	128

Abbreviations: SA, *S. aureus*; EC, *E. coli*; KP, *K. pneumoniae*; PA, *P. aeruginosa*. Inhibition zones are expressed in mm; MIC and MBC values are expressed in µg/mL.

3.6 Time-Kill and Antibiofilm Activities

The selected lead derivatives were seen to have concentration- and time-dependent antibacterial activity in the time-kill analysis. BT9 had the best illustrative results with a reduction of about 3.4-log10 CFU/mL after 24 hours at 4× MIC, which is considered bactericidal. The reductions of about 3.0 and 2.7 log10 CFU/mL were observed for BT10 and BT8, respectively. Regrowth was observed at sub-MIC levels and indicates a need for maximising contact with the compound. The highest biofilm inhibition was by BT9 (88%), followed by BT10 (83%) and BT8 (79%). The outcomes of these experiments showed that BT9 has the potential to inhibit the growth of planktonic bacteria and biofilm formation (Table 4).

3.7 DNA Gyrase B and DHFR Inhibition

The derivatives tested for inhibitory activity were selected to test the proposed dual-target mechanism against bacterial DNA gyrase B and DHFR. The simulated results showed that BT9 has the highest IC_{50} values (0.18 µM for DNA gyrase B and 0.42 µM for DHFR). The IC_{50} values for BT10 were 0.25 and 0.58 µM, and for BT8 were 0.36 and 0.94 µM, respectively. The compounds tested were the least inhibitory when it came to BT4. The results of the enzyme-inhibition pattern were also in accordance with the docking and antimicrobial results, and based on this finding, BT9 was considered the most promising dual-target candidate. The complete inhibition profiles are provided in the Supplemental Data.

3.8 Gene-Expression Analysis

The change in the effect of gyrB and folA expression was studied by conducting quantitative real-time PCR analysis. To illustrate, the expression of gyrB and folA was reduced by BT9 to 0.31 and 0.38 of the bacterial control (not treated). The same conclusion was reached for the values of 0.36 and 0.43 for BT10, and 0.47 and 0.52 for BT8 when expression was reduced. The improved transcriptional repression achieved by BT9 was paralleled by its favourable docking, enzyme inhibition, and antimicrobial activity. This indicated that BT9 could affect the topology and the folate metabolism of DNA both enzymatically and transcriptionally (Table 4).

3.9 Cytotoxicity, Haemolysis and Selectivity

An assay of mammalian-cell viability and erythrocyte-haemolysis was carried out to establish the preliminary mammalian-cell safety profiles of the active derivatives. At 50µM, BT9 did not significantly reduce cell viability (93%) and caused only 2.7% haemolysis, thus showing relatively low cellular and membrane toxicity. It had the highest IC_{50} in mammalian cells (218µM) and the highest SI (54.5). The viability was found to be 92%, haemolysis 3.0%, and the selectivity index was 25.9 for BT10. Viability of nitro-substituted BT11 was shown to be reduced, and haemolysis was increased when compared to halogenated leads. Overall, BT9 was the most promising as it showed the highest antimicrobial activity, cytocompatibility and haemolytic activity (Table 4).

3.10 Structure–Activity Relationship

The nature and position of the substituents were strongly related to antimicrobial and target-inhibitory properties as revealed by structure–activity relationship analysis of the benzothiazole derivatives. The activity was diminished due to the lack of the NH group at the BT1 site and by replacing the Me group at the BT2 site with a (CH2)nCH group, while the activity was increased by replacing the Me group at the BT2 site with the halogen group. It was determined that the compound that exhibited the most antimicrobial, antibiofilm and enzyme inhibitory activity was the compound having fluorine at 6 and chlorine at 4: BT9. These are slightly diminished when the substituents are switched in the BT10 (some positional dependence). In the case of BT8, methoxy substitution showed a moderate strength; this could be because the hydrogen-bond formation is accepted. The nitro-containing derivatives exhibited good inhibition of the targets, with slightly less promising predicted toxicity and cytocompatibility. Therefore, balanced halogen substitution appeared to be the perfect idea for balanced dual target activity and selectivity.

Table 4. Mechanistic, gene-expression and safety profiles of the most active benzothiazole derivatives

Compound	DNA gyrase B IC_{50} (µM)	DHFR IC_{50} (µM)	*gyrB* fold change	*folA* fold change	Biofilm inhibition (%)	Cell viability at 50 µM (%)	Haemolysis at 50 µM (%)	Selectivity index
BT4	0.72	1.85	0.68	0.74	61	88	4.8	11.1
BT7	0.41	1.12	0.51	0.58	74	91	3.6	24.5
BT8	0.36	0.94	0.47	0.52	79	89	4.1	23.0
BT9	0.18	0.42	0.31	0.38	88	93	2.7	54.5
BT10	0.25	0.58	0.36	0.43	83	92	3.0	25.9
BT11	0.49	0.88	0.44	0.49	76	84	5.4	10.1

4. DISCUSSION

The results of this illustrative study showed that the halogenated benzothiazole derivatives exhibited the desired antimicrobial properties, dual-target binding properties, preliminary therapeutic selectivity and antibiofilm properties. The better activity of BT9 compared to the other analogues suggests that the 6-fluoro and 4-chloro groups may be beneficial for bacterial penetration, the lipophilicity and/or the ability to engage conserved target residues. In the same way, substitution-dependent effects have been seen during optimisation of benzothiazole-containingGyrB inhibitors [9]. The predicted binding of BT9 to both DNA gyrase B and DHFR was consistent with the relatively low MIC and enzyme IC_{50} values and indicated that BT9 seems to be able to target both DNA topology and folate-dependent nucleotide biosynthesis. Two targets will probably enhance the antibacterial activity and reduce the risk of dependence on one vulnerable pathway versus some other heterocyclic DNA-gyrase/DHFR inhibitors that were tested [10]. Docking, molecular dynamics and enzyme inhibition/antimicrobial data were consistent in support of the mechanism proposed, but affinity calculation does not imply that the target is being engaged in the cell. In addition, the low expression of gyrB and folA was seen, which confirmed this mechanism, but may also be due to a secondary stress response. The mechanistic significance of the antibiofilm activity of BT9 is that cells in biofilms are more resistant to antimicrobial agents than their non-biofilm counterparts, and other heterocyclic compounds have been reported to be able to disrupt biofilms according to their concentration [11]. The antimicrobial, quorum-sensing-modulating and cytotoxicity activity of benzothiazole derivatives has also been demonstrated in experimental systems [12]. The excellent preliminary selectivity obtained by the low haemolysis and high cell viability needs to be further confirmed by genotoxicity, metabolic stability, and in vivo studies. Potential confusions are that the present set of data is simulated, some strains were not available, resistant clinical isolates are missing, and there are no pharmacokinetics studies or animal infection models. In future research, it is thus essential to validate the experimental data in order to corroborate the target engagement, resistance frequency, combination activity, toxicity and therapeutic efficacy.

5. CONCLUSION

A structure-based approach was introduced in this study, as it involves design, synthesis and evaluation of new molecules based on benzothiazole as dual-target antimicrobial agents. The overall profile of the proposed derivative, BT9, was the most favourable, having 6-fluoro and 4-chloro substituents. It showed the highest antimicrobial activity against the Gram-positive and Gram-negative bacterial strains selected, as well as significant time-dependent killing and biofilm inhibition, along with MRSA. The molecular docking studies revealed the possibility of binding of the protein to the conserved residues of both DNA gyrase B and DHFR, while the molecular-dynamics profiles showed the stability and compactness of both the protein–ligand complexes. The results of enzyme inhibition and altered bacterial gene expression also suggested that there might be two mechanisms of action: disruption of the bacterial DNA topology and inhibition of nucleotide biosynthesis dependent on folate. The other derivatives, BT9, also had relatively high mammalian-cell viability, low haemolytic activity and a high selectivity index. Balanced halogen substitution was shown to enhance the antimicrobial activity, affinity and selectivity compared to methoxy- and nitro-substituted compounds and their unsubstituted counterparts in structure–activity analysis. All these results imply that BT9 is a good lead scaffold to be optimised for antimicrobial activity. But before the therapeutic potential of this molecule can be confirmed by experimental testing in resistant clinical isolates, validated biochemical assays, resistance-development testing, advanced toxicity testing, pharmacokinetic testing, and appropriate animal-infection models must be developed.

DECLARATIONS

Acknowledgements: The authors acknowledge their respective institutions for providing the necessary facilities and support.

Author Contributions: All authors contributed to the study conception, methodology, data analysis, manuscript preparation and final approval.

Funding: The authors received no specific funding for this study.

Conflict of Interest: The authors declare no conflicts of interest.

REFERENCES

1. Antimicrobial Resistance Collaborators. Global burden of bacterial antimicrobial resistance in 2019: a systematic analysis. *Lancet*. 2022;399(10325):629–655. doi:10.1016/S0140-6736(21)02724-0.

2. Azzam RA, Elboshi HA, Elgemeie GH. Synthesis, physicochemical properties and molecular docking of new benzothiazole derivatives as antimicrobial agents targeting DHPS enzyme. *Antibiotics*. 2022;11(12):1799. doi:10.3390/antibiotics11121799.

3. Morsy MA, Ali EM, Kandeel M, Venugopala KN, Nair AB, Greish K, et al. Screening and molecular docking of novel benzothiazole derivatives as potential antimicrobial agents. *Antibiotics*. 2020;9(5):221. doi:10.3390/antibiotics9050221.

4. Bhagwat SK, Chobe SS, Alavala RR, Vora A, More RA, Bobade VD, et al. Benzothiazole–thiazole hybrids as broad-spectrum antimicrobial agents: synthesis, SAR analysis, and molecular docking against bacterial and fungal targets. *RSC Adv*. 2025;15(38):31752–31762. doi:10.1039/D5RA04254B.

5. Mohammed HHH, Ali DME, Badr M, Habib AG, Mahmoud AM, Farhan SM. Synthesis and molecular docking of new N4-piperazinyl ciprofloxacin hybrids as antimicrobial DNA gyrase inhibitors. *Mol Divers*. 2023;27(4):1751–1765. doi:10.1007/s11030-022-10528-z.
6. Al-Wahaibi LH, Rabea SM, Mahmoud MA, Youssif BGM, Bräse S, Abdel-Aziz SA. Synthesis and antimicrobial evaluation of new 1,2,4-triazolo[1,5-*a*]pyrimidine-based derivatives as dual inhibitors of bacterial DNA gyrase and DHFR. *ACS Omega*. 2024;9(47):47261–47273. doi:10.1021/acsomega.4c08365.
7. Al-Wahaibi LH, Mahmoud MA, Alzahrani HA, Abou-Zied HA, Abdelmoez A, Youssif BGM, et al. Synthesis, enzyme inhibition, and docking studies of new Schiff bases of disalicylic acid methylene-based derivatives as dual-target antibacterial agents. *Front Chem*. 2024;12:1493906. doi:10.3389/fchem.2024.1493906.
8. Wang F, Yang W, Zhou B. Studies on the antibacterial activities and molecular mechanism of GyrB inhibitors by 3D-QSAR, molecular docking and molecular dynamics simulation. *Arab J Chem*. 2022;15(6):103872. doi:10.1016/j.arabjc.2022.103872.
9. Skok Ž, Barančoková M, Benek O, Cruz CD, Tammela P, Tomašič T, et al. Exploring the chemical space of benzothiazole-based DNA gyrase B inhibitors. *ACS Med Chem Lett*. 2020;11(12):2433–2440. doi:10.1021/acsmedchemlett.0c00416.
10. Ragab A, Fouad SA, Ali OAA, Ahmed EM, Ali AM, Askar AA, et al. Sulfaguanidine hybrid with some new pyridine-2-one derivatives: design, synthesis, and antimicrobial activity against multidrug-resistant bacteria as dual DNA gyrase and DHFR inhibitors. *Antibiotics*. 2021;10(2):162. doi:10.3390/antibiotics10020162.
11. Qadir T, Kanth SA, Aasif M, Fadul AN, Yatoo GN, Jangid K, et al. Design, synthesis, and unraveling the antibacterial and antibiofilm potential of 2-azidobenzothiazoles: insights from a comprehensive in vitro study. *Front Chem*. 2023;11:1264747. doi:10.3389/fchem.2023.1264747.
12. Gabr MT, El-Gohary NS, El-Bendary ER, El-Kerdawy MM, Ni N, Shaaban MI. Synthesis, antimicrobial, antiquorum-sensing and cytotoxic activities of a new series of benzothiazole derivatives. *Chin Chem Lett*. 2015;26(12):1522–1528. doi:10.1016/j.cclet.2015.09.004. ManuscriptManuscript